



## Deep Ultraviolet-to-NIR Broad Spectral Response Organic Photodetectors with Large Gain

|                               |                                                                                                                                                                                                                                                                                                                                                                                                                                                                                                                                                                                                                                                       |
|-------------------------------|-------------------------------------------------------------------------------------------------------------------------------------------------------------------------------------------------------------------------------------------------------------------------------------------------------------------------------------------------------------------------------------------------------------------------------------------------------------------------------------------------------------------------------------------------------------------------------------------------------------------------------------------------------|
| Journal:                      | <i>Journal of Materials Chemistry C</i>                                                                                                                                                                                                                                                                                                                                                                                                                                                                                                                                                                                                               |
| Manuscript ID                 | TC-ART-12-2015-004188.R1                                                                                                                                                                                                                                                                                                                                                                                                                                                                                                                                                                                                                              |
| Article Type:                 | Paper                                                                                                                                                                                                                                                                                                                                                                                                                                                                                                                                                                                                                                                 |
| Date Submitted by the Author: | 04-Feb-2016                                                                                                                                                                                                                                                                                                                                                                                                                                                                                                                                                                                                                                           |
| Complete List of Authors:     | <p>Yang, Dezhi; Changchun Institute of Applied Chemistry, State Key Laboratory of Polymer Physics and Chemistry<br/>         Zhou, Xiaokang; Changchun Institute of Applied Chemistry, Chinese Academy of Sciences<br/>         wang, Yanping; Changchun Institute of Applied Chemistry, Chinese Academy of Sciences<br/>         Vadim, Agafonov; Moscow Institute of Physics and Technology,<br/>         Alshehri, Saad M.; King Saud University, Department of Chemistry, College of Science<br/>         Ahamad, Tansir; King Saud University, Chemistry<br/>         Ma, Dongge; Changchun Institute of Applied Chemistr, Polymer Chemistry</p> |



## Deep Ultraviolet-to-NIR Broad Spectral Response Organic Photodetectors with Large Gain

Received 00th January 20xx,  
Accepted 00th January 20xx

Dezhi Yang,<sup>a</sup> Xiaokang Zhou,<sup>a</sup> Yanping Wang,<sup>a</sup> Agafonov Vadim,<sup>\*b</sup> Saad M. Alshehri,<sup>c</sup> Tansir Ahamad,<sup>c</sup> and Dongge Ma<sup>\*a,c</sup>

DOI: 10.1039/x0xx00000x

[www.rsc.org/](http://www.rsc.org/)

We developed organic photodetectors with high photocurrent gain by enhancing the electron tunneling from the electrode owing to the effect of interface charge trapping. Furthermore, we utilized a down-conversion material to enhance the photoresponse in the deep-ultraviolet (UV) range. As a result, the photodetectors achieved an external quantum efficiency (EQE) of as high as 4000% while the photoreponsivity remains 9 A/W at the UV wavelength of 250 nm. Finally, a broad-photoresponse high-performance organic photodetector covering a spectral range from deep-UV (200 nm) to near-infrared (1000 nm) was successfully realized. The maximum EQE exceeds 10000% at a wavelength of 780 nm, and the photoreponsivity and specific detectivity are up to 70 A/W and  $4 \times 10^{12}$  Jones, respectively.

### Introduction

The detection of light from ultraviolet (UV) to near-infrared (NIR) spectral range is a technology in demand for many applications, including imaging, communications, remote control, environmental monitoring, and chemical/biological sensing.<sup>[1–3]</sup> However, traditional inorganic photodetectors show relatively narrow response spectra. Recently, organic photodetectors have shown broad-spectral-response properties.<sup>[4]</sup> Considerable effort has been made to synthesize materials and design device structures to construct organic photodetectors with broad spectral response.<sup>[5–9]</sup> However, the photoresponse in deep-UV and NIR ranges is still relatively low because of the UV light absorption of the substrate and electrode and the insufficient exciton separation in the organic layer. Thus, an effective method for solving these problems is imperative.

A method employed to solve the low photo response in the deep-UV range is using a thin layer of aluminum as a semi-transparent electrode,<sup>[10–12]</sup> which can help UV light reach the active layer. However, the response in the visible range will be reduced because of the visible-light absorption of aluminum. Another method is using quartz glass as substrate and

conductive electrode, such as PEDOT:PSS, which does not have UV absorption.<sup>[13]</sup> However, the use of quartz glass instead of ordinary glass increases the cost. Moreover, flexible devices are also difficult to realize. Accordingly, we introduce in this paper a more advantageous strategy to address this issue. Given that large-bandgap organic materials can absorb UV light and emit visible light, we can use this down-conversion process to convert the UV light into a photocurrent. At the same time, the visible light can pass through the layer of large-bandgap organic material to form a photocurrent. Thus, the devices can respond to light from the deep-UV–NIR range. The photon-to-current conversion efficiency of organic photodetectors can be improved by constructing a device with a large photoconductive gain, which facilitates the enhancement of the photoresponse in the NIR range.<sup>[14–20]</sup> Therefore, high-response organic photodetectors capable of broad-spectrum detection can be achieved by combining the aforementioned two methods.

In this paper, we report organic photodetectors with both high gain and broad spectral response from deep-UV–NIR range. In our devices, a thin interfacial charge-trapping layer is introduced to enhance the electron tunneling from the electrode, thus significantly increasing the photocurrent gain, and a wide-bandgap organic material, 4P-NPB, is used as the down-conversion layer to extend the spectral response to deep-UV light. The resulting organic photodetectors show high photoresponse in the wide spectral range of 250–1000 nm. Their external quantum efficiency (EQE) is over 1000% in the spectral range of 250–900 nm, and the maximum EQE exceeds 10000% at a wavelength of 780 nm.

<sup>a</sup> State Key Laboratory of Polymer Physics and Chemistry, Changchun Institute of Applied Chemistry, Chinese Academy of Sciences, Changchun 130022, P. R. China

\*E-mail: [mda1014@ciac.ac.cn](mailto:mda1014@ciac.ac.cn)

<sup>b</sup> Moscow Institute of Physics and Technology, Dolgoprudny, Moscow region, 141700, Russia

\*E-Mail: [aqvadim@yandex.ru](mailto:aqvadim@yandex.ru)

<sup>c</sup> Department of Chemistry, King Saud University, Riyadh, 11451, Kingdom of Saudi Arabia

## Experimental

TPBi, LiF, TAPC, SnPc, BCP, and C70 were purchased from Sigma-Aldrich without further purification. The devices were fabricated by the thermal evaporation of the organic materials on indium–tin–oxide (ITO)-coated glass substrates each with a sheet resistance of 10  $\Omega$ /sq. Prior to deposition, the substrate was thoroughly cleaned in an ultrasonic bath using detergents and de-ionized water successively. The pure and doped organic films were deposited under high-vacuum condition (pressure < 10<sup>-4</sup> Pa). The thickness was controlled in situ by a quartz crystal monitor and calibrated by Dektak 6M Profiler (Veeco). Aluminum electrodes were deposited on the organic films through shadow masks. The active area of each device was 16 mm<sup>2</sup>. All the measurements were performed under ambient condition.

For quantum-efficiency measurement, a setup by 7-Star Optical Instruments Co., Ltd., Beijing was used. The incident light from a halogen lamp (250 W) passing through a monochromator was chopped at 160 Hz and focused on the active areas of the devices. The photocurrent signal was first amplified using a low-noise current amplifier (DLPCA-200, Femto) and then detected by a lock-in amplifier (SR830, Stanford Research Systems). The reverse biases on the devices were obtained using Keithley 236 Source-Measure Unit. A crystalline silicon photodiode (S1337-1010BQ, Hamamatsu) calibrated by the National Institute of Metrology of China was used as a reference before each measurement.

## Results and discussion

Only few free charge-carriers exist in organic semiconductors. The charge carriers, which form current in organic semiconductors, are usually injected from the electrodes. An injection method is tunneling injection. However, the injected current through tunneling injection is affected by the width and height of the potential barrier together with the occupied energy states and unoccupied energy states in the electrode and semiconductor. If the free-charge carriers generated by the light could be used to enhance tunneling injection from the electrode, a high photoconductive gain should be obtained. Thus, we could increase the EQE of the organic photodetectors by this method.

In this study, we designed an effective device structure to realize large-electron tunneling injection and consequently successfully fabricate organic photodetectors with high photoconductive gain. The device structure and the diagram of its schematic energy level are shown in Figure 1. A thin hole-blocking layer and a hole-accumulation layer of C70 are introduced onto the side of ITO cathode. The hole-blocking layer may be organic electron-transporting molecules with a large bandgap, such as TPBi and BmPyPB, and may use interface insulators, like LiF. A wide-bandgap electron-transporting molecule, BCP, is inserted between the aluminum electrode and the active layer, which consists of TAPC and C70 blends, to avoid the injection of electrons from the aluminum

anode. Therefore, under dark condition, the electrons and holes are difficult to inject into the active layer because of the blocking layers at the electrode interfaces. However, under light condition, the excitations are generated in the TAPC:C70 active layer and then separated and transported toward the electrodes under external electric field. A large amount of holes are accumulated in the C70 layer by the hole blocking layer, resulting in a considerable voltage drop in TPBi; thus, the width of the barrier to electron tunneling injection from the ITO electrode is significantly reduced because of band bending. In this case, a large amount of electrons are injected into the device from the ITO cathode. Therefore, the device produces a large photocurrent; as a direct result, the EQE values of the devices are greatly enhanced. The detailed structure of the organic photodetectors fabricated are ITO\TPBi(3 nm)\C70(10 nm)\TAPC:C70(70 nm)\BCP(10 nm)\Al, ITO\BmPyPB (3 nm)\C70(10 nm)\TAPC:C70(70 nm)\BCP(10 nm)\Al and ITO\LiF (3 nm)\C70(10 nm)\TAPC:C70(70 nm)\BCP(10 nm)\Al. Figure 2(a), (b), and (c) show the EQE properties of the organic photodetectors with 3 nm TPBi, BmPyPB, and LiF hole-blocking layers, respectively. The EQE values of all three devices exceed 100% and reach 1000% in the spectral range of 200–700 nm at over -4 V bias. The maximum EQE even exceeds 10000%. This result also indicates that TPBi, BmPyPB, and LiF all play effective blocking functions in hole accumulation and electron tunneling. Obviously, the increase in EQE should be attributed to the large tunneling of electrons resulting from the hole accumulation at the interface via light. In fact, we found that the structure of our device with LiF as hole-blocking layers is similar with the Metal-insulator-semiconductor (MIS) in traditional inorganic device<sup>[21]</sup>. The ITO, LiF and C70 behaves like metal, the insulator and semiconductor, respectively. And the thickness of LiF is 3 nm, which is just in the range from 1 nm to 5nm of insulator layers in MIS devices. Moreover, the small difference between the work function of ITO around 4.8 eV and LUMO of C70 about 4.6 eV is beneficial to the electron tunneling injection from the ITO. According to the book of Physics of Semiconductor Devices authored by S. M. Sze, the relation between the current density and voltage can write to Equation 1,<sup>[21]</sup> As shown in Figure 2(d), the current density-voltage characteristics of the three devices exhibit a linear behavior in semi-logarithmic plots; this trend is well in accordance with the equation of tunneling current (Equation 1), further proving that the large electron current is indeed due to the tunneling of electrons.

$$J = A^* T^2 e^{(-\alpha_T \phi_T^{1/2} d)} e^{-q\phi_B / kT} (e^{qV / kT} - 1) \quad (1)$$

where  $A^*$  is the effective Richardson constant,  $T$  is the temperature,  $\alpha_T = 2(2m^*/\hbar^2)$ ,  $m^*$  is effective mass,  $\hbar$  is the reduced Planck constant,  $\phi_T$  is the effective barrier height for tunneling,  $d$  is thickness of insulator layer,  $q$  is the absolute value of electron charge ( $1.6 \times 10^{-19}$  coulombs),  $\phi_B$  is the barrier height,  $k$  is Boltzmann constant.

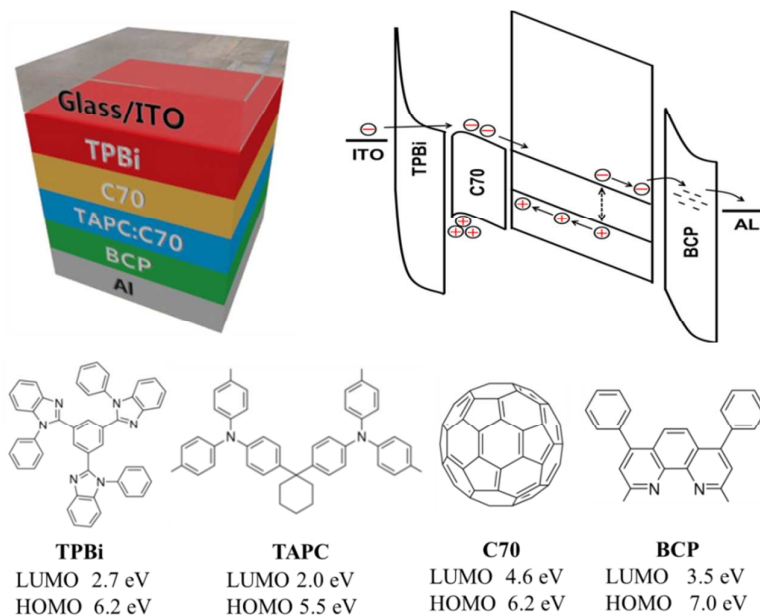


**Figure 1.** Structure and schematic energy level diagram of the fabricated organic photodetectors. The schematic diagram of the energy-level alignment under work condition are given, including the processes of hole accumulation and electron injection. The chemical structures of organic materials used in this study together with the lowest unoccupied molecular orbital (LUMO) and the highest occupied molecular orbital (HOMO) are shown at the bottom.

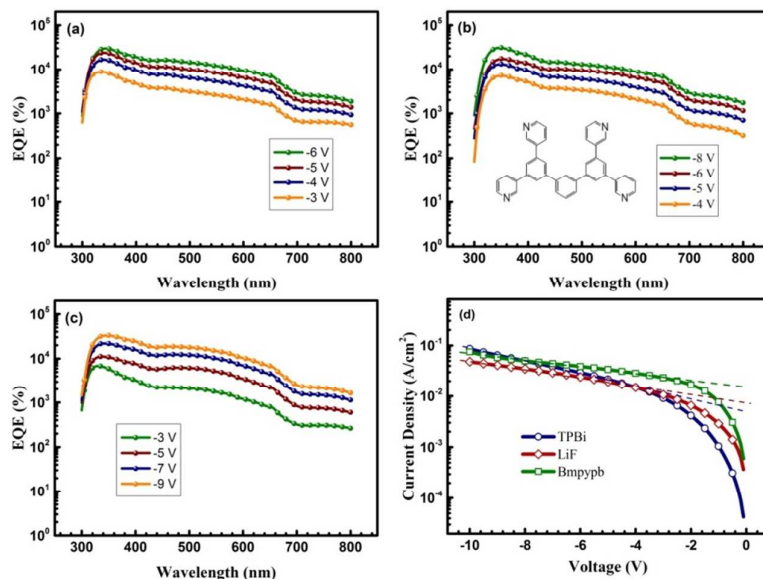


**Figure 2** EQE properties of devices (a) ITO\TPBi(3 nm)\C70(10 nm)\TAPC:C70(70 nm)\BCP(10 nm)\Al, (b) ITO\Bmppyb(3 nm)\C70(10 nm)\TAPC:C70(70 nm)\BCP(10 nm)\Al and the inset shows the chemical structure of Bmppyb, and (c) ITO\LiF(3 nm)\C70(10 nm)\TAPC:C70(70 nm)\BCP(10 nm)\Al. Current density–voltage characteristics of the three devices are shown in (d), in which the fitting curves by Equation 1 are also given.



## Journal of Materials Chemistry C

## ARTICLE

When TAPC:C70 is adopted as the active layer limits the photoresponse in the wavelength range of 300–800 nm. To broaden the wavelength photoresponse, we use SnPc with NIR light absorption capacity to replace TAPC to fabricate the photodetectors. The detailed structure of the organic photodetectors fabricated is ITO/TPBi (3 nm)/C70 (10 nm)/SnPc:C70 (70 nm)/BCP (10 nm)/Al. Figure 3(a) shows the EQE properties of the fabricated devices at different bias voltages. Clearly, the wavelength response is extended to 1000

nm. The EQE is over 100% in the wavelength range of 300–950 nm. The maximum EQE can reach 10000% at a wavelength of 780 nm and –8 V bias. This result also indicates that the device structure we designed is also suitable for narrow-bandgap materials. As shown in Figure 3(b), the current density–voltage characteristic of the fabricated device based on SnPc:C70 is similar to that of the device based on TAPC:C70, indicating that the high photocurrent gain in this narrow bandgap-based device results from the electron tunneling.

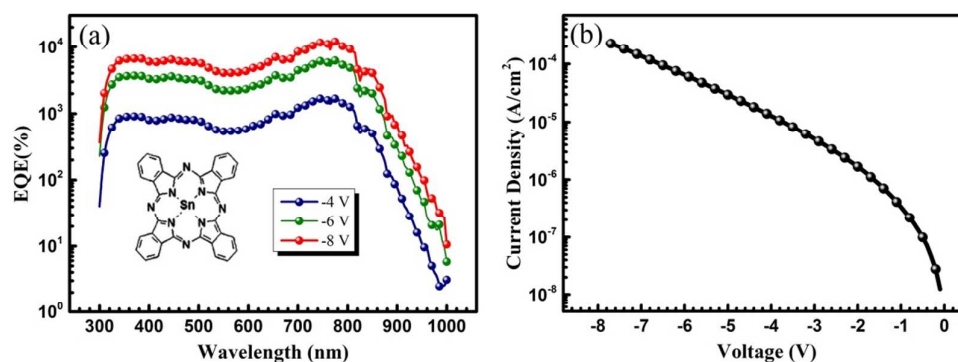


**Figure 3.** (a) EQE properties of the photodetectors with ITO/TPBi (3 nm)/C70 (10 nm)/SnPc:C70 (70 nm)/BCP (10 nm)/Al architecture under different bias conditions. The chemical structure of SnPc is also shown. (b) Current density–voltage characteristic of the photodetectors under dark condition.

To achieve a broad spectral response device, we covered the surface of glass with a thin layer 4P-NPB of 200 nm to enhance the photoresponse in the deep-UV range.<sup>[22–23]</sup> The detailed structure of the organic photodetectors fabricated is 4P-NPB (200 nm)/Glass/ITO/TPBi (3 nm)/C70 (10 nm)/SnPc:C70 (70 nm)/BCP (10 nm)/Al. A diagram of the work principle is shown in Figure 4(a). When the UV light irradiates the 4P-NPB, the device will absorb the light and emit visible light. The generated visible light will then reach the photoactive layer, finally converting the UV light into the photocurrent. The results are shown in Figure 4(c). Notably, the response range can indeed extend to the deep-UV light wavelength of 250 nm, and the response wavelength should be able to extend well to 200 nm if our EQE test setup is not limited in measured wavelength. To the best of our knowledge, this should be the

highest EQE value for deep-UV organic photodetectors. The photodetectors we fabricated show a wide spectral response property ranging from 200 nm to 1000 nm. The maximum EQE is higher than 10000% at 780 nm. If we assume that the shot noise from the dark current is the major contribution, the specific detectivity can be expressed as  $D^* = R/(2qJ_d)^{1/2}$ , where  $R$  is the responsivity,  $q$  is the absolute value of the electron charge ( $1.6 \times 10^{-19}$  coulombs), and  $J_d$  is the dark current density. As shown in Figure 4(d), the specific detectivity is calculated to be over  $10^{11}$  Jones in the wavelength range of 200–1000 nm, and the maximum value reaches  $4 \times 10^{12}$  Jones at a 780 nm wavelength and –10 V bias. These results are comparable to those of well-established inorganic silicon photodetectors. The specific responsivity also reaches 70 A/W at 780 nm wavelength and –10 V bias.

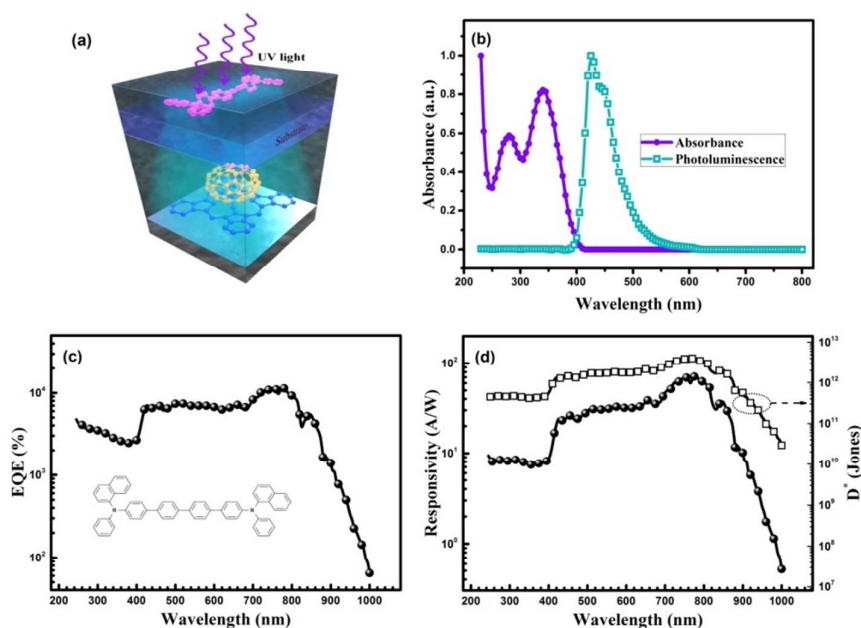


**Figure 4.** (a) Schematic diagram of down-conversion organic photodetectors. (b) Absorption and photoluminescence spectra of 200 nm neat 4P-NPB film on quartz. (c) EQE property of the photodetector with 4P-NPB (200 nm)/Glass/ITO/TPBi (3 nm)/C70 (10 nm)/SnPc:C70 (70 nm)/BCP (10 nm)/Al architecture at  $-10$  V bias. The chemical structure of 4P-NPB is also given. (d) Responsivity and detectivity properties of the down-conversion photodetector at  $-10$  V bias.

## Conclusions

We designed high-gain organic photodetectors with a wide spectral response from the deep-UV wavelength of 200 nm to the NIR wavelength of 1000 nm. The EQE values of the resulting photodetectors are significantly increased in a wide spectral range by enhancing the electron tunneling from the electrode owing to the effect of interface charge trapping. The UV wavelength response is also greatly enhanced by introducing a down-conversion UV light absorption layer. The maximum EQE exceeds 10000% at the wavelength of 780 nm, and the corresponding values of photoresponsivity and specific detectivity are up to 70 A/W and  $4 \times 10^{12}$  Jones, respectively. Actually, the organic photodetectors could further extend the photoresponse wavelength to a wider range by adopting longer-wavelength NIR materials, along with high gain. Owing to the high-response performances of the fabricated organic photodetectors in an extremely wide wavelength range, they could be applied to a various applications, including imaging, communication, and defense.

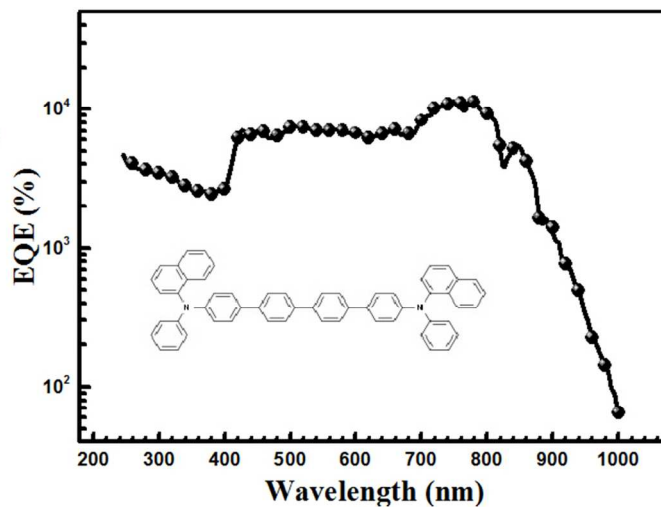
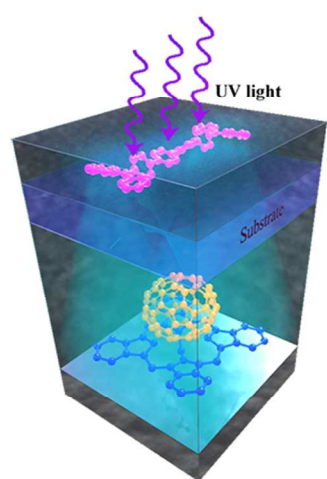
## Acknowledgements

The authors gratefully acknowledge the International Cooperation Foundation of China (2015DFR10700), the National Natural Science Foundation of China (51403203, 61204059) and the Basic Research Project of Jilin Province (20150520018JH) for the support of this research, also this work was partly supported by Russian Ministry of Education and Science - state assignment № 3.1579.2014/K. Prof. D. G. Ma extends his appreciation to the Distinguished Scientist Fellowship Program (DSFP) at King Saud University, Riyadh, Kingdom of Saudi Arabia for financial support.

## Notes and references

1. E. H. Sargent, *Advanced Materials*, 2005, **17**, 515-522.
2. A. Rogalski, J. Antoszewski and L. Faraone, *J Appl Phys*, 2009, **105**, 091101.
3. S. Kim, Y. T. Lim, E. G. Soltesz, A. M. De Grand, J. Lee, A. Nakayama, J. A. Parker, T. Mihaljevic, R. G. Laurence, D. M.

- Dor, L. H. Cohn, M. G. Bawendi and J. V. Frangioni, *Nat Biotechnol*, 2004, **22**, 93-97.
4. X. Gong, M. H. Tong, Y. J. Xia, W. Z. Cai, J. S. Moon, Y. Cao, G. Yu, C. L. Shieh, B. Nilsson and A. J. Heeger, *Science*, 2009, **325**, 1665-1667.
  5. Y. Yao, Y. Y. Liang, V. Shrotriya, S. Q. Xiao, L. P. Yu and Y. Yang, *Advanced Materials*, 2007, **19**, 3979.
  6. Y. J. Xia, L. Wang, X. Y. Deng, D. Y. Li, X. H. Zhu and Y. Cao, *Appl Phys Lett*, 2006, **89**, 081106.
  7. L. S. Li, Y. Y. Huang, J. B. Peng, Y. Cao and X. B. Peng, *J Mater Chem C*, 2014, **2**, 1372-1375.
  8. Y. Dong, W. Z. Cai, M. Wang, Q. D. Li, L. Ying, F. Huang and Y. Cao, *Org Electron*, 2013, **14**, 2459-2467.
  9. J. D. Zimmerman, E. K. Yu, V. V. Diev, K. Hanson, M. E. Thompson and S. R. Forrest, *Org Electron*, 2011, **12**, 869-873.
  10. S. H. Wu, W. L. Li, B. Chu, C. S. Lee, Z. S. Su, J. B. Wang, F. Yan, G. Zhang, Z. Z. Hu and Z. Q. Zhang, *Appl Phys Lett*, 2010, **96**, 093302.
  11. F. Yan, H. H. Liu, W. L. Li, B. Chu, Z. S. Su, G. Zhang, Y. R. Chen, J. Z. Zhu, D. F. Yang and J. B. Wang, *Appl Phys Lett*, 2009, **95**, 253308.
  12. H. G. Li, G. Wu, H. Z. Chen and M. Wang, *Org Electron*, 2011, **12**, 70-77.
  13. L. Zhu, Q. Dai, Z. F. Hu, X. Q. Zhang and Y. S. Wang, *Opt Lett*, 2011, **36**, 1821-1823.
  14. J. Reynaert, V. I. Arkhipov, P. Heremans and J. Poortmans, *Adv Funct Mater*, 2006, **16**, 784-790.
  15. I. H. Campbell and B. K. Crone, *Appl Phys Lett*, 2009, **95**, 263302.
  16. F. C. Chen, S. C. Chien and G. L. Cious, *Appl Phys Lett*, 2010, **97**.
  17. S. T. Chuang, S. C. Chien and F. C. Chen, *Appl Phys Lett*, 2012, **100**, 013309.
  18. W. T. Hammond and J. G. Xue, *Appl Phys Lett*, 2010, **97**, 073302.
  19. H. Y. Chen, M. K. F. Lo, G. W. Yang, H. G. Monbouquette and Y. Yang, *Nat Nanotechnol*, 2008, **3**, 543-547.
  20. F. W. Guo, B. Yang, Y. B. Yuan, Z. G. Xiao, Q. F. Dong, Y. Bi and J. S. Huang, *Nat Nanotechnol*, 2012, **7**, 798-802.
  21. S. M. Sze, *Physics of Semiconductor Devices* (Second Edition), 1998, p547.
  22. G. Schwartz, S. Reineke, T. C. Rosenow, K. Walzer and K. Leo, *Adv Funct Mater*, 2009, **19**, 1319-1333.
  23. G. Schwartz, M. Pfeiffer, S. Reineke, K. Walzer and K. Leo, *Advanced Materials*, 2007, **19**, 3672.



80x39mm (300 x 300 DPI)